Progress in Nuclear Energy 103 (2018) 209–216

Contents lists available at ScienceDirect

Progress in Nuclear Energy

journal homepage: www.elsevier.com/locate/pnucene

Three-dimensional experiment of heat transfer for molten oxidic pool

Lian Chen[a,*], Kun Han[a], Tao Li[a], Daogui Tian[a], Ying Chen[a], Huajian Chang[a,b], Xinchen Xu[a], Jie Pei[a], Jinlong Zhang[a], Tao Zhang[a]

[a] *State Nuclear Power Technology R&D Center, South Park Future Science and Technology Campus, Beijing 102209, China*
[b] *Institute of Nuclear and New Energy Technology, Tsinghua University, Beijing 10084, China*

ARTICLE INFO

Keywords:
Heat transfer
Oxidic pool
Severe accident
Experiment

ABSTRACT

The effectiveness of in-vessel retention (IVR) of core melt during severe accident in light water reactor strongly depends on whether the heat removed from boundaries could exceed the heat generated in the molten pool in lower head of reactor pressure vessel (RPV). Natural convection in the oxidic pool plays a key role in determining the heat transfer behavior inside the molten pool. A Molten pool Oxide-layer heat tRaNsfer experiment (MORN) facility was built to investigate the heat transfer characteristic of the molten oxidic pool with the intention to verify the heat transfer correlation of the pool. The test facility consists of a three dimensional hemisphere test section with an inner radius of 0.4 m. The outer boundary of the test section could be cooled by different methods (radiation or convection), so as to study the influence of external cooling condition on the crust formation of oxidic pool. Three kinds of material have been chosen as the simulants. They are water, $NaNO_3/KNO_3$(mole ratio 1:4) and a non-eutectic binary mixture of calcium-boron oxide (30 wt%CaO-70 wt% B_2O_3) respectively. At first period, several water and salt experiments with the melt height of 340 mm were performed and the data were analyzed. Though the normalized temperature distribution of the pool was nearly the same between water and salt experiments, the heat flux across the side wall differed much. The heat flux distribution of the water experiment rose nearly linearly with polar angle till to the melt surface. The heat flux of salt experiment at the low angle was larger than that of water, decreased slightly with angle increasing and then rose quickly till to the melt surface. This is consistent with the LIVE and COPRA experiments with the same boundary condition. The maximum normalized heat flux of the water experiment was approximate 1.6 and that of the salt experiment was about 2.2. The downward heat transfer of MORN is smaller than the correlation derived by COPO, mini-ACOPO and BALI experiments, but is consistent as LIVE, COPRA experiment.

1. Introduction

In-vessel retention of core melt is regarded as being able to reduce the risk of large scale radioactive released to the containment and correspondingly to the environment. It is believed that IVR is an important severe accident management strategy and has been adopted by some nuclear power plants in operation as well as some advanced reactors (Theofanous et al., 2002; Kymäläinen et al., 1997; Park et al., 2001). But the effectiveness of IVR strongly depends on whether the heat removed from boundaries could exceed the heat generated in the melt pool. The heat transfer during the severe accident involves complex physical and chemical phenomena of a postulated accident sequence in the RPV. Since the database for the severe accident transient is still very limited, bounding condition method is employed which supposes steady state of molten pool in the lower head has been achieved. The molten pool in the lower head is likely to be regarded as two parts: metal pool at the top, consisting of liquid steel or Zirconium, and the oxidic pool at the bottom, mainly consisting of UO_2 and ZrO_2 (Asmolov et al., 2001), as shown in Fig. 1. The decay heat of melt generated in the oxidic pool is transferred by natural circulation upward to the metal pool and to the coolant of ERVC through side wall (Park et al., 2006). Then the heat transferred to the metal pool is transferred upward to the internal of RPV by radiation and to side wall by natural circulation. Whether the heat flux to side wall would exceed the critical heat flux outside of RPV is believed to be the most important criterion of determining the integrity of RPV and the success of IVR strategy after the molten pool is formed, especially for the higher power reactor (Theofanous et al., 1996). This heat flux distribution relies on many aspects, such as melt pool constitution and configuration, internal decay power, external boundary conditions of RPV, top condition of the pool, crust configuration and so on. For the natural convection with internal heat generation, the heat transfer is characterized by the

* Corresponding author.
E-mail address: chenlian@snptc.com.cn (L. Chen).

https://doi.org/10.1016/j.pnucene.2017.11.014
Received 22 October 2016; Received in revised form 8 November 2017; Accepted 21 November 2017

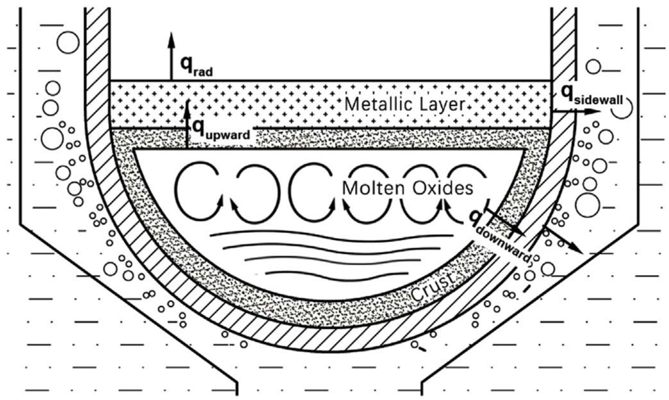

Fig. 1. Illustration of the natural convection flow and stratification patterns in the oxidic pool.

Nusselt number (*Nu*) in terms of modified Rayleigh (*Ra*') number, Prandtl (*Pr*) and geometry parameter. It is usually expressed as follow:

$$Nu = CRa'^{a}e^{b}\mathrm{Pr}^{C} = C\left(\frac{g\beta q_v H^5}{\lambda\nu\alpha}\right)^{a}\left(\frac{H}{R}\right)^{b}\left(\frac{\nu}{\alpha}\right)^{c} \quad (1)$$

The modified *Ra*' is correlated with Grashof (*Gr*), Dammkohler (*Da*) number and *Pr* number:

$$Gr = \frac{g\beta\Delta tH^3}{\nu^2} \quad Da = \frac{q_v H^2}{\lambda\Delta t} \quad (2)$$

In which, q_v is the volumetric heat generation rate, and α, λ, ν and β are the melt thermal diffusivity, thermal conductivity, kinematic viscosity and thermal expansion coefficient, respectively. *H* is the characteristic length of the molten pool.

Due to the complex thermal-hydraulic phenomena of the oxidic pool heat transfer, in the past decades, several facilities have been established and various experiments have been performed to study the law of the thermal hydraulics in corium pools (Mayinger et al., 1976; Asmolov et al., 2001), including the upward and downward heat transfer. These experiments were performed with different geometries (mainly 2D and seldom 3D), different simulant (mainly water, solution, Freon and few salt liquid) under different boundary conditions and covered different ranges of Rayleigh number that characterizes the melt pool natural convection, as shown in Table 1. It is known that the *Pr* for corium pools is in the range of 0.4–1.2 and *Ra'* in order of 10^{16} (Vieira et al., 2014). It is a significant technical challenge to perform experiments with prototypical molten-core material, since temperature is about 3000 K. In order to reach the 10^{16} order of Ra', some experiments were carried out with water and freon as simulant fluids (Theofanous et al., 1996), with much lower temperature and *Pr* in the range of 2–10. Correlations are derived from these different experiments which are shown in Table 2 (Theofanous et al., 1996). These correlations were applied to develop severe accident heat transfer models in the lower head for analysis. But uncertainty of the heat flux distribution and downwards heat transfer varies widely among correlations or experimental data. Fig. 2 shows the Nu_{dn}-*Ra*' relationship of some experiments and Fig. 3 gives the heat flux curve obtained from some experiments (Zhang et al., 2016a). In Fig. 3, θ_{max} means the polar angle corresponding to the pool upper surface, q_{local} stands for the local heat flux at polar angle θ and q_{mean} is the averaged heat flux. Obvious discrepancy was observed from the figures and there lacks assured conclusion on the reason, which indicates the complexity to research the molten pool phenomena and the need of more experiment with different boundary condition.

More understanding of the heat transfer in oxidic pool can help to accurately evaluate the IVR strategy of the PWR. The MORN facility was established and experiments were done to study the heat transfer characteristic of the molten oxidic pool. Three kinds of simulant will be used in the experiment: the widely used water, the non-eutectic binary mixture same with the LIVE facility and the non-eutectic binary oxide mixture. Furthermore, the influence of power density and cooling condition on pool temperature field, heat flux distribution and crust formation were also investigated. At present, eight tests were performed with the intention to verify the correlation about the heat flux of oxidic pool as well as study the cooling condition effect on core melt progression in the RPV after the core melt relocated into the lower plenum.

2. Experiment description

2.1. Experiment facility

The experiment facility consists of a test section, a furnace, an instrument & control system and a cooling system, as shown in Fig. 4.

The test section comprises of a semi-spherical vessel and a cylinder section, which is made of specialized stainless steel that sustains long time at high temperature. The inner diameter of the vessel is 800 mm which represents a 1: 5 scaled lower head of a typical pressurized water reactor vessel. The height of the cylinder part is 50 mm with the thickness of 30 mm. A flow path with width of 100 mm is formed at the outside of the test section to enable external cooling with either water or air. The coolant enters the flow path from inlets at the bottom of the cooling vessel and leaves from 8 pipes located at the top, which are evenly distributed along the circumference (Fig. 5). A specialized structure was set near the bottom to enable pouring out the working fluid after experiment for reusing of the test section. Spiral water-cooling copper tube was installed to provide upper cooling of the

Table 1
Experiments performed recently on oxidic pool heat transfer.

Test Facility	Simulant	Size	Ra'	*Pr*	Boundary condition	Heating method
COPO (Kymäläinen et al., 1994)	$ZnSO_4$-H_2O	0.8 × 1.77 × 0.1 m (2D)	1.24e14–1.66e15	2–3	Water cooled	Direct heat
mini-ACOPO (Theofanous and Liu, 1995)	Freon R-113	Φ0.44 m (3D)	2e13-7e14	2.6–10.8	Water cooled	Transient cooldown
UCLA (Asfia and Dhir, 1996)	Freon R-113	Φ60.6 m (3D)	2e10-1.1e14	8	Water cooled	Micro wave
ACOPO (Theofanous et al., 1997)	Water	Φ2m (2D)	1e14-1e16	1.7–8.6	Water cooled	Transient cooldown
SIMECO (Sehgal et al., 1998)	Water/olefin/Glycerol/ Benzyl benzoate	Φ0.5 m (2D)	9.6e12-9.5e13	–	Water cooled	Direct heating
BALI (Bonnet and Seiler, 1999)	water	R = 2 m (2D)	1e15-1e17	2.6–10.8	Liquid Nitrogen, Crust formed	Electrode mesh
RASPLAV-A (Asmolov et al., 2000)	NaF/$NaBF_4$	Φ0.4 m (2D)	2.7e11–1.36e15	5.07–7.73	Water/air cooled, Crust formed	Direct heating
LIVE (Gaus-Liu et al., 2010)	$NaNO_3$/KNO_3	Φ1m (3D)	1e10-1e11	1–6.4	Water/air cooled, Crust formed	Direct heating
COPRA (Zhang et al., 2016)	Water and $NaNO_3$/KNO_3	R2.2 m (2D)	1.18e15-4e16	1–6.4	Water cooled	Direct heating